Published in final edited form as:
Brain Res. 2011 November 24; 1425: 132–141. doi:10.1016/j.brainres.2011.09.052.

Probing ischemic tissue fate with BOLD fMRI of brief oxygen challenge

Qiang Shen, **Shiliang Huang**, **Fang Du**, and **Timothy Q Duong**
Research Imaging Institute, [2]Departments of Ophthalmology, Radiology, and Physiology, University of Texas Health Science Center, South Texas Veterans Health Care System, San Antonio, TX

Abstract

It has been recently shown that at-risk tissue exhibits exaggerated T_2^*-weighted MRI signal increases during transient oxygen challenge (OC), suggesting that the tissue is still metabolically active. This study further characterized the effects of transient OC on T_2^*-weighted MRI in permanent focal stroke rats (N=8) using additional quantitative measures. The major findings were: *i*) the ischemic core cluster showed no significant response, whereas the mismatch cluster showed markedly higher percent changes relative to normal tissue in the acute phase. *ii)* Many of the mismatch pixels showed exaggerated OC responses, which eventually became infracted. The area with exaggerated OC responses was larger than the mismatch, suggesting that some tissue with reduced diffusion were potentially at risk. *iii*) Basal T_2^*-weighted intensities on the perfusion-diffusion contourplot were high in normal tissue and low in the core, with a sharp transition in the mismatch. *iv*) OC-induced changes on the perfusion-diffusion contourplot dropped monotonously for pixels below perfusion and diffusion viability thresholds. *v*) Basal T_1 increased slightly in the ischemic core ($P<0.05$). OC decreased T_1 in normal ($P<0.05$) but not in mismatch and core pixels. *vi*) OC decreased CBF in normal ($P<0.05$) but not in mismatch and core pixels. T_2^*-weighted MRI of OC has the potential to offer unique clinically relevant data.

Keywords

MRI; perfusion; diffusion; oxygen inhalation; penumbra

1. INTRODUCTION

The ability to distinguish reversible from irreversibly damaged ischemic brain tissue is of clinical importance in deciding treatment strategies for acute stroke patients. The gold standard to define ischemic penumbra (i.e., salvageable tissue) is by imaging oxygen extraction fraction using positron emission tomography which unfortunately is not widely available and involves ionized irradiation (Baron, 1999). A more commonly used imaging modality to define the ischemic penumbra is the diffusion-perfusion mismatch by MRI (Schlaug et al., 1999). However, some mismatch tissue is oligemic, salvageable and other is not salvageable, depending on the duration and nature of ischemic injury, and proximity of

Correspondence: Timothy Q Duong, PhD, University of Texas Health Science Center at San Antonio, Research Imaging Institute, 8403 Floyd Curl Dr, San Antonio, TX 78229. Phone: 210 567 8100, Fax: 210 567 8152, duongt@uthscsa.edu.

patent vessels, among others. Thus, the perfusion-diffusion mismatch only approximates the ischemic penumbra. Despite its shortcomings (Kidwell et al., 2003), the perfusion-diffusion mismatch remains widely utilized to guide acute stroke treatment in the clinical settings. Numerous studies have attempted to probe the fate of the mismatch to improve prediction accuracy of the ischemic tissue fate.

A novel approach was recently introduced to further probe tissue at risk by using T_2^*-weighted MRI of transient oxygen challenge in ischemic stroke (Dani et al., 2010; Santosh et al., 2008). T_2^*-weighted signal intensity is sensitive to relative concentration of deoxyhemoglobin (Ogawa and Lee, 1990; Ogawa et al., 1993). The infarct core showed little or no change in T_2^*-weighted signal intensity during oxygen challenge (OC). The at-risk regions surrounding the infarct core showed an exaggerated increase in OC T_2^*-weighted signal intensity compared to the homologous region in the contralateral hemisphere. OC brings in oxygenated blood displacing the high deoxyhemoglobin concentration in the at-risk region where cerebral blood flow (CBF) is partially compromised but its metabolic activity remains significant. It was thus hypothesized that tissue with exaggerated increase in T_2^*-weighted signal intensity during OC is potentially salvageable (Dani et al., 2010; Santosh et al., 2008).

The goal of this study was to further characterizing the OC T_2^*-weighted signal responses in the permanent focal stroke rats by using additional and quantitative measures. The ischemic core, normal and mismatch were objectively classified pixel-by-pixel using automated cluster analysis based on quantitative apparent diffusion coefficient (ADC) and CBF (Shen et al., 2004b). Basal T_2^*-weighted signal intensities, magnitude and percent signal changes due to oxygen challenges, and their times to peaks were analyzed for the three tissue types. These data were also evaluated as a function of binned ADC and/or CBF on a pixel-by-pixel basis. Moreover, ischemia-induced and OC-induced T_1 changes were analyzed to evaluate their potential effects on CBF and T_2^*-weighted signals in stroke animals.

2. RESULTS

Figure 1 shows the ADC, CBF, OC T_2^*-weighted percent-change maps at 30 mins, and T_2-weighted MRI at 24 hrs after permanent MCAO from one animal and all animals. ADC and CBF were reduced in the stroke hemisphere as expected. ISODATA – iterative self-organizing data analysis – used clustering analysis and classified pixels into normal, mismatch and core clusters. The ischemic core pixels showed a mixture of low positive and negative percent changes. Mismatch cluster showed regions of markedly higher percent changes compared to the homologous region in the contralateral hemisphere. The exaggerated OC responses are most consistent and apparent in the primary somatosensory cortex (solid long arrows) and less apparent in brain structures along the midline (dash short arrows). The area with exaggerated OC response was larger than the ISODATA mismatch area which eventually became infracted at 24 hrs as shown by T_2-weighted MRI at 24 hrs. In the normal hemisphere, there were some exaggerated OC responses which were likely from large vessels as indicated by their shapes. These vessels could be readily identified.

The OC response time courses from all animals showed that the mismatch OC response was about twice that of the normal OC response, and the core cluster showed negligible OC response (Figure 2A). Time to peak of the mismatch was significantly delayed compared to normal tissue. Group-averaged OC percent changes, TTP, ADC and CBF values for the three types of tissues were quantified and are summarized in Figure 2B. Group-averaged OC percent changes were significantly different among all three tissue types ($P < 0.05$). Mismatch OC % change was 1.5 times higher than normal OC % changes and the core OC

% change was 3.5 times smaller than normal. Mismatch TTP was about 2.5 times longer than normal TTP.

In addition, basal T_2^*-weighted signal, OC-induced magnitude changes and OC-induced percent changes were analyzed as a function of ADC and CBF at 30 mins after stroke (Figure 3). The vertical solid lines and shaded bars indicate, respectively, normal values of ADC and CBF and their standard deviations obtained from this study. Two vertical dot lines and the shaded bars indicate, respectively, the viability thresholds and their standard deviations as reported in (Shen et al., 2003). T_2^*-weighted signal intensities of normal ADC and CBF were generally high (Fig 3A). There was a sharp transition in basal T_2^*-weighted signal intensities between the two vertical lines. For ADC and CBF below the viability thresholds, T_2^*-weighted signal intensities was low and relatively independent of ADC and CBF. Figure 3B and *C* show that the OC-induced changes in pixels with ADC and CBF below their viability thresholds were markedly reduced. By contrast, pixels with ADC and CBF between normal and viability thresholds showed markedly higher changes than those of normal tissue.

The OC responses were also analyzed on the combined ADC-CBF contour plot with color-code scale indicating baseline T_2^*-weighted signal intensities, OC magnitude changes, and OC percent changes (Figure 4, 30 mins after MCAO). Baseline T_2^*-weighted signal intensities of the mismatch were lower than normal, and those of the ischemic core were lower than mismatch. The OC magnitude and percent changes of the mismatch were markedly higher than normal, whereas those of the core were negligible. There were some distinct differences between OC magnitude- and percent-change contour plots in that the peak of the percent-change responses were localized to the mismatch zone on the contourplot whereas the peak of the magnitude-change responses were also located at a relatively higher CBF values. In the OC magnitude change plot, the largest changes centered about 0 ml/g/min and 0.55×10^{-3} mm^2/s as well as 0.3 ml/g/min and 0.65×10^{-3} mm^2/s. By contrast, in the OC % change plot, the largest changes centered about 0 ml/g/min and 0.55–0.65×10^{-3} mm^2/s. Note that a few negative CBF pixels in Figure 4 were due to subtraction errors in the continuous ASL technique for CBF close to zero (Shen et al., 2003).

The effects by ischemia and OC on T_1 and CBF changes were analyzed for the 30-min time point after stroke (Figure 5). Basal T_1 increased slightly in the ischemic core (8 ± 2%). OC decreased T_1 significantly ($P < 0.05$) in the normal hemisphere (1.8 ± 0.8%), but not in ischemic core (−0.2 ±0.2%) and mismatch (−0.6 ± 1.0%). OC decreased CBF significantly in the normal hemisphere (0.15 ± 0.07 ml/gram/min, 16 ± 8%) ($P < 0.05$), but had no significant effect on the core and mismatch tissue. Although OC responses on sham rats were not measured, our previous data on normal animals subjected to OC challenges were not statistically different from the normal hemisphere of stroke rats herein (data not shown).

3. DISCUSSION

This study further characterized of the effects of transient oxygen challenge on T_2^*-weighted signal intensities in permanent stroke rats. The major findings were: *i*) the ischemic core cluster, derived automatically from perfusion and diffusion data, showed no significant response, whereas the mismatch cluster showed markedly higher percent changes relative to normal tissue in the acute phase. The exaggerated OC responses are most apparent in the primary somatosensory cortex and less apparent in other brain structures in this animal stroke model. *ii)* Many of the mismatch pixels showed some exaggerated OC responses, which eventually became infracted. *iii*) Basal T_2^*-weighted signal intensities on the perfusion-diffusion contourplot were high in the normal cluster and low in the core cluster, with a sharp transition in the mismatch cluster. *iv*) OC-induced magnitude and percent

changes on the perfusion-diffusion contourplot dropped monotonously for pixels below perfusion-diffusion viability thresholds. *v*) Basal T_1 increased slightly in the ischemic core. OC decreased T_1 significantly in the normal hemisphere, indicative of hyperoxia-induced vasoconstriction or increased dissolved oxygen in the plasma, but OC had no significant T_1 effect in the ischemic core and mismatch pixels. *vi*) OC decreased CBF significantly in the normal hemisphere, but had no significant CBF effect on the mismatch and the ischemic core pixels.

The present study corroborated Santosh's findings (Santosh et al., 2008) in the following ways. In normal tissue, the increased oxygen delivery during OC resulted in increased T_2^*-weighted signal intensities because capillary and venous oxygenation still have some rooms for increased oxygen saturation. In the ischemic core, there was no blood-flow and no oxygen delivery and thus OC T_2^*-weighted change was negligible. In the mismatch, some tissue was still metabolically active but with restricted blood flow, and thus oxygen extraction fraction and deoxyhemoglobin concentration in the capillaries and veins were higher than normal. Upon OC, T_2^*-weighted signal magnitude increased in the mismatch was higher than in normal tissue. The exaggerated OC % changes were likely because of the smaller denominator. Blood gas O2 saturation was ~90% under air and 100% under oxygen inhalation. Thus, the T_2^*-weighted signal changes were unlikely to come from the arterial compartment; rather they came from the venous compartment.

The present study also extended Santosh's study in several ways. First, it probed the OC response in the normal, mismatch and ischemic core clusters that were objectively defined. Second, basal T_2^*-weighted signal intensities and magnitude change of OC and the response time to peak were analyzed as a function of ADC or CBF on a pixel-by-pixel basis as well as the ADC-CBF contour plots. Results were interpreted with respect to the ADC and CBF viability thresholds. Third, the potential effects on T_2^*-weighted signal responses by ischemia and OC were analyzed. These results are discussed below.

3.1. OC responses in ischemic core, normal and mismatch

The OC % map showed that many of the ISODATA-defined mismatch pixels had exaggerated OC responses compared to normal pixels (Figure 1), whereas the ischemic core had no significant OC responses. We avoided ROI analysis because it could unintentionally bias as there were considerable heterogeneous T_2^*-weighted signal changes across the brain. A case in point is that even within the normal hemisphere, there were small areas that had high or low OC responses (Figure 1) due to large vessels or white matter, respectively. The advantage of the cluster analysis is that these clusters include all pixels within the three defined classes, which improved certainty and demonstrated that most mismatch pixels exhibited exaggerated OC responses. In some animals, the area with exaggerated OC response was larger than the mismatch area, suggesting that some tissue with reduced ADC were at risk and thus potentially salvageable. ISODATA analysis showed that pixels with exaggerated OC responses eventually became infracted in permanent stroke.

The exaggerated OC response was often found in the primary somatosensory cortex. We believe that the anterior communicating artery offers collateral flow and thus the primary somatosensory cortex is among the few structures that have a better chance of being salvaged by reperfusion. This is consistent with the variable and higher than normal CBF and ADC in this region compared to many subcortical regions. Moreover, unlike the hypoperfused regions in the subcortical regions which have embedded large vessels, the OC response in primary somatosensory was not contaminated by large vessels, which made the high OC response in primary somatosensory region easily visible. It is interesting to note that the TTP of OC response was longer in mismatch tissue. The longer TTP of OC response in the mismatch tissue was due to delayed delivery of oxygen in a manner similar to TTP in

dynamic contrast susceptibility CBF measurement. As such the TTP of OC response could potentially be used to identify at risk tissue.

Some of the scattered core pixels had moderately high OC response (Figure 2B), likely due to some residual oxygen delivery and/or minor contamination by non-core pixels. There were no significant differences in baseline CBF or ADC between pixels with and without OC response in the core.

There are some confounds in this study. Although ISODATA can include analysis of all pixels within the three defined classes, its disadvantage is that there could be misclassified pixels. Another confound is that some pixels in the normal hemisphere showed exaggerated OC responses. Similar high OC response patterns were also seen in normal rats. The high OC response in the contralateral hemisphere was most likely from contamination by vessels. By doing pixel-by-pixel normalization using the contralateral hemisphere response as control, exaggerated OC responses could also be detected. Not all mismatch pixels showed exaggerated OC responses. This could be because the mismatch and exaggerated OC responses depicted different physiological status, although it is possible there were minor cluster classification errors. Further studies are needed to compare the tissue fate of the mismatch and exaggerated OC responses (i.e., to evaluate the tissue fate with reperfusion).

3.2. OC responses as a function of ADC and CBF

There was also considerable heterogeneity of ADC and CBF within each tissue cluster. We thus analyzed the basal T_2^*-weighted signal intensities, magnitude and percent change by OC as a function of ADC alone and CBF alone, and with respect to viability thresholds (Shen et al., 2003). For pixels below ADC and CBF viability threshold (Figure 3), basal T_2^*-weighted signal intensities were low and constant, whereas OC % changes drop from high to low rapidly with decreasing ADC or CBF. The likely explanation is that, at sufficiently low ADC and CBF, the occlusion essentially occluded the vessel and tissue oxygenation is completely hypoxic without oxygen gradient under basal (air) conditions. By contrast, an oxygen gradient was likely present in pixels with mildly reduced ADC which were likely close to patent vessels. Reduced T_2-weighted signals have been observed to vary among infarct core, penumbra and normal tissue (Kavec et al., 2001; Kavec et al., 2004). However, sensitivity is low precluding practical application of basal T_2^*-weighted MRI to identify salvageable and non-salvageable tissue.

For pixels with ADC and CBF above the viability thresholds but below normal values, basal T_2^*-weighted signal intensities decreased progressively with decreasing ADC or CBF, whereas the OC changes were higher than normal pixels. The ADC and CBF values of tissue with enhanced OC responses were above the ADC and CBF viability thresholds (Meng et al., 2004; Shen et al., 2003), supporting the notion that pixels with exacerbated OC responses were at risk tissue and thus potentially salvageable. These observations further corroborate the significances of viability thresholds established previously under similar experimental conditions (Meng et al., 2004; Shen et al., 2003).

Note that baseline T_2^*-weighted intensities at the high ends of the ADC and CBF values continued to rise slightly instead of reaching a plateau. The high ADC is likely due to contamination by cerebrospinal pixels and the high CBF is likely due to contamination of pixels with high vascular density. OC-induced responses however showed a plateau (Figure 3BC). These high ADC and CBF pixels could be readily distinguished on maps.

Although the information from OC responses as a function of ADC or CBF alone were informative, it was incomplete and was even misleading because these plots did not take into accounts the CBF status for each ADC bin and vice versa. A case in point is that the peak of

the contour plots (Figure 4B) is localized at 0 ml/g/min and 0.55×10^{-3} mm^2/s whereas peaks appeared at 0.6 ml/g/min and 0.6×10^{-3} mm^2/s (Figure 3B). This discrepancy was the result of mixing normal and low CBF pixels in Figure 3B, shifting the OC response peaks. Thus, the OC responses on the CBF-ADC contour plots should be more accurate because they accounted for both tissue ADC and CBF properties.

Careful inspection of the ADC-CBF contour plots showed there were some distinct differences in OC magnitude and percent changes. The peaks of the exaggerated OC changes tended to be at lower CBF in the % contour plot, likely because of the division by smaller basal T_2^*-weighted signal intensities. This raises the question whether magnitude changes should be used instead. While the OC percent changes may be biased by the low basal T_2^*-weighted signal, it may be more sensitive. Additional studies are needed to determine which analysis method will provide more accurate prediction of final infarct volume (Huang et al., 2011). With improved MRI sensitivity, the ability of basal T_2^* or T_2-weighted MRI to identify salvageable and non-salvageable tissue may be warrant.

3.3. T_1 effects on OC responses

In this study, the TR (1 s with 60° flip angle) was not infinitely long and thus, there could be T_1-weighting in the T_2^*-weighted signals. There are two potential T_1 effects on OC-induced T_2^*-weighted signal changes: *i)* T_1 induced by ischemia, and *ii)* T_1 induced by dissolved molecular oxygen during OC. In the acute phase (up to 3 hrs) during which vasogenic edema in the permanent MCAO is likely minimal, the ischemia-induced T_1 change is likely small, as indeed the case herein. In the chronic stroke phase during which edema could be significant (Tanaka et al., 2010, in press), longer T_1 due to edema effect in cerebral ischemia would result in a reduced OC response.

Oxygen inhalation increased dissolved paramagnetic molecular oxygen decreases T_1 in normal tissue. Oxygen delivery and consumption might differ among the three different tissue types, the T_1 effect by dissolved oxygen could vary among the tissue types. In the core, this was not an issue because there was no oxygen delivery and OC-induced % changes were low. In the normal tissue, dissolved oxygen due to OC decreased T_1, which exaggerated T_2^*-weighted OC response for short TR. In the mismatch tissue, OC increases dissolved oxygen somewhat (but less than normal) and, thus, augmented T_2^*-weighted signal for short TR but to a less extent than in normal tissue. That said, with a 60° flip angle and 1 s TR, these effects were likely small for all tissue types in the permanent MCAO model in the acute phase.

In normal tissue, OC decreased CBF by 16 ± 8% due to hyperoxia-induced vasoconstriction, consistent with the ~10% hyperoxia-induced CBF reduction reported previously (Kety and Schmidt, 1948; Sicard and Duong, 2005). In the mismatch, OC increased instead of decreased CBF likely because the vessels were either damaged and did not experience significant hyperoxia. The improved oxygenation by OC could also improve perfusion (Henninger et al., 2007; Shin et al., 2007). Dissolved O_2 may change blood T_1 and the brain T_1, which could affect CBF calculation. This effect on CBF calculation, although unknown, is likely small. Some studies have shown that prolonged oxygen inhalation in cerebral ischemia to be beneficial (Henninger et al., 2007; Shin et al., 2007) while other studies have shown it to be harmful (Michalski et al., 2010; Padma et al., 2011). The beneficial effects include reversal of ADC lesion, prolongation of the mismatch status, extending the therapeutic window. The harmful effects include increased generation of reactive oxygen species. The brief (2 mins) OC herein, it is unlikely to significantly alter ischemic tissue fate. A short OC duration can be used in future studies to avoid potential unwanted effects on ischemic tissue fate.

In summary, this study presents further characterization of the effects of transient oxygen challenge on T_2^*-weighted signal intensities in stroke rats as function of ADC and CBF on a pixel-by-pixel basis. The key finding is that many of the perfusion-diffusion mismatch shows exaggerated oxygen-challenge responses. Future studies will evaluate the effects of treatment (such as reperfusion) on the exaggerated OC responses, quantitatively define the OC-response viability threshold, and employ predictive model to determine if exaggerated OC responses improves prediction accuracy.

4. EXPERIMENTAL PROCEDURE

4.1. Animal preparation

Animal experiments were performed with approval of the Institutional Animal Care and Use Committee**,** UT Health Science Center San Antonio. Eight male Sprague Dawley rats (250–300g) were anesthetized with 2% isoflurane in air during surgery. Permanent focal brain ischemia of the right hemisphere was induced using the intraluminal middle cerebral artery occlusion (MCAO) method (Shen et al., 2003). Animals were mechanically ventilated and maintained at ~1.2% isoflurane in air during MRI (unless otherwise perturbed by OC). End-tidal CO2 was monitored via a Surgivet capnometer (Smith Medical, Waukesha, WI, USA). Noninvasive end-tidal CO2 values have been calibrated previously against invasive blood-gas samplings under identical settings (Sicard et al., 2003). The rectal temperature was maintained at 37.0 ± 0.5° C. The heart rate and blood oxygen saturation level were monitored using a MouseOx system (STARR Life Science Corp., Oakmont, PA, USA). All recorded physiological parameters were maintained within normal physiological ranges unless otherwise perturbed by OC.

Quantitative CBF and ADC were acquired every 30 mins post-occlusion up to 180 mins. Transient oxygen challenge (inhaling oxygen) was performed at about 45 mins post-occlusion. T_2^*-weighted MRI was performed during which the animals breathed 1 mins air, 2 mins O_2, 5 mins air, and 2 mins O_2, and 2 mins air. To evaluate the possible effects of ischemia and OC on T_1 and CBF which could indirectly affect T_2^*-weighted signal changes during OC, quantitative T_1 and CBF were measured during air and during oxygen inhalation (6 mins). These additional T_1 and CBF measurements were performed on some animals (n = 5). All rats were imaged again at 24-hr post-occlusion and T_2 maps were acquired to confirm infarct volume.

4.2. MRI experiments

MRI experiments were performed on a 7-T/40-cm magnet, a Biospec Bruker console (Billerica, MA), and a 40-G/cm gradient insert (ID = 12 cm, 120-μs rise time). A surface coil (2.3-cm ID) was used for brain imaging and a neck coil (Duong et al., 2000) for perfusion labeling. Coil-to-coil electromagnetic interaction was actively decoupled.

ADC—Averaged ADC was obtained by averaging three ADC maps with diffusion-sensitive gradients separately applied along the x, y or z direction. Single-shot, spin-echo echo-planar images (EPI) were acquired (Shen et al., 2005) with matrix = 96 × 96 with partial Flourier (5/8) acquisition and reconstructed to 128 × 128, FOV = 2.56 × 2.56 cm, seven 1.5-mm slices, TR = 3 s (90° flip angle), TE = 37 ms, b = 4 and 1200 s/mm^2, Δ = 17.53 ms, δ = 5.6 ms, and 16 averages.

CBF—CBF was measured using the continuous arterial spin-labeling (cASL) technique with single-shot, gradient-echo, echo-planar-imaging (EPI) acquisition as described previously (Shen et al., 2005). Continuous arterial spin labeling employed a 2.7-s square radiofrequency pulse to the labeling coil. Acquisition parameters were matrix = 96 × 96 with

partial Flourier (5/8) acquisition and reconstructed to 128 × 128, FOV = 2.56 × 2.56 cm, seven 1.5-mm slices, TR = 3 s (90° flip angle), and TE = 10.2 ms,

T_2^*-weighted MRI of oxygen challenge—OC fMRI was acquired using T_2^*-weighted gradient-echo EPI, matrix = 96 × 96 (reconstructed to 128 × 128), FOV = 2.56 × 2.56 cm, seven 1.5-mm slices, TR = 1 s, TE = 26 ms, 60° flip angle. OC experiment paradigm was: 1 min OFF, 2 mins ON, 5 mins OFF, 2 mins ON and 1 min OFF, and 720 repetitions in total.

T_1—T_1-weighted images were acquired using single-shot inversion-recovery gradient-echo EPI sequence with 6 different inversion delay times (0.025, 0.5, 1, 2, 4 and 8 s), matrix = 96 × 96 (reconstructed to 128 × 128), FOV = 2.56 × 2.56 cm, TR = 12 s (90° flip angle), and 4 signal averages.

T_2—T_2-weighted images were acquired using fast spin-echo pulse sequence with two effective echo times (50 and 80ms), TR = 2s (90° flip angle), matrix = 128 × 128, FOV = 2.56 × 2.56 cm, echo train length 8, and 8 signal averages.

4.3. Data analysis

Data analysis used codes written in Matlab (MathWorks Inc., Natick, MA, USA) and the STIMULATE (University of Minnesota) software. Data were reported as mean ± SD, with $P < 0.05$ (t-test) taken to be statistically significant. ADC, CBF and T_2 maps were calculated as described previously (Shen et al., 2003; Shen et al., 2004a). OC response percent change maps with respect to basal (air) conditions were calculated. T_1 maps with intensity in unit of seconds were calculated pixel-by-pixel by $S_i = S_0 - 2Ae^{-TI_i/T1}$ where Si is the signal intensity obtained with inversion delay time TI_i.

Cerebrospinal fluid and the corpus callosum were excluded from analysis via ISODATA method (Shen et al., 2004b). Three tissue types (normal, perfusion-diffusion mismatch and ischemic core) were characterized by using auto-clustering ISODATA method (Shen et al., 2004b) based on ADC and CBF data. Images among different animals were co-registered using custom-designed semi-automatic co-registration software (Liu et al., 2004; Schmidt et al., 2006; Shen et al., 2005; Shen and Duong, 2008) to generate group-averaged maps. Percent change, time to peak (TTP), ADC and CBF values were analyzed for different tissue types for individual animals, followed by group averaging. Time to peak was defined as the time from one standard deviation above the mean of baseline to 90% of the mean peak value.

Profiles of baseline T_2^*-weighted signal intensity, OC signal magnitude change, and OC percent change were plotted as function of ADC or CBF. Baseline T_2^*-weighted signal intensity, signal intensity change by OC and OC percent changes were also plotted on ADC-CBF contour plots. The grid size was 0.02×10^{-3} mm^2/sec for ADC or 0.12 mL/gram/min for CBF, respectively. Data were interpreted with respect to viability thresholds (Shen et al., 2003).

T_1 and CBF changes induced by oxygen were analyzed for the ISODATA determined ischemic core, mismatch and compared with the homologous regions in the contralateral hemisphere.

Acknowledgments

This work was supported by the NIH (R01-NS45879), the American Heart Association (EIA 0940104N and SDG 0830293N) and Clinical and Translational Science Awards (parent grant UL1RR025767).

References

Baron JC. Mapping the ischaemic penumbra with PET: implications for acute stroke treatment. Cerebrovasc Dis. 1999; 9:193–201. [PubMed: 10393405]

Dani KA, Santosh C, Brennan D, McCabe C, Holmes WM, Condon B, Hadley DM, Macrae IM, Shaw M, Muir KW. T2*-weighted magnetic resonance imaging with hyperoxia in acute ischemic stroke. Ann Neurol. 2010; 68:37–47. [PubMed: 20582987]

Duong TQ, Silva AC, Lee SP, Kim SG. Functional MRI of calcium-dependent synaptic activity: cross correlation with CBF and BOLD measurements. Magn Reson Med. 2000; 43:383–92. [PubMed: 10725881]

Henninger N, Bouley J, Nelligan JM, Sicard KM, Fisher M. Normobaric hyperoxia delays perfusion/diffusion mismatch evolution, reduces infarct volume, and differentially affects neuronal cell death pathways after suture middle cerebral artery occlusion in rats. J Cereb Blood Flow Metab. 2007; 27:1632–42. [PubMed: 17311078]

Huang S, Shen Q, Duong TQ. Quantitative prediction of acute ischemic tissue fate using support vector machine. Brain Res. 2011; 1405:77–84. [PubMed: 21741624]

Kavec M, Grohn OH, Kettunen MI, Silvennoinen MJ, Penttonen M, Kauppinen RA. Use of spin echo T(2) BOLD in assessment of cerebral misery perfusion at 1.5 T. MAGMA. 2001; 12:32–9. [PubMed: 11255090]

Kavec M, Grohn OH, Kettunen MI, Silvennoinen MJ, Garwood M, Kauppinen RA. Acute cerebral ischemia in rats studied by Carr-Purcell spin-echo magnetic resonance imaging: assessment of blood oxygenation level-dependent and tissue effects on the transverse relaxation. Magn Reson Med. 2004; 51:1138–46. [PubMed: 15170833]

Kety SS, Schmidt CF. The effects of altered arterial tensions of carbon dioxide and oxygen on cerebral blood flow and cerebral oxygen consumption of normal young men. J Clin Invest. 1948; 27:484–491.

Kidwell CS, Alger JR, Saver JL. Beyond mismatch: evolving paradigms in imaging the ischemic penumbra with multimodal magnetic resonance imaging. Stroke. 2003; 34:2729–35. [PubMed: 14576370]

Liu ZM, Schmidt KF, Sicard KM, Duong TQ. Imaging oxygen consumption in forepaw somatosensory stimulation in rats under isoflurane anesthesia. Magn Reson Med. 2004; 52:277–285. [PubMed: 15282809]

Meng X, Fisher M, Shen Q, Sotak CH, Duong TQ. Characterizing the diffusion/perfusion mismatch in experimental focal cerebral ischemia. Ann Neurol. 2004; 55:207–12. [PubMed: 14755724]

Michalski D, Hartig W, Schneider D, Hobohm C. Use of normobaric and hyperbaric oxygen in acute focal cerebral ischemia - a preclinical and clinical review. Acta Neurol Scand. 2010; 123:85–97. [PubMed: 20456243]

Ogawa S, Lee TM. Magnetic resonance imaging of blood vessels at high fields: in vivo and in vitro measurements and image simulation. Magn Reson Med. 1990; 16:9–18. [PubMed: 2255240]

Ogawa S, Menon RS, Tank DW, Kim S-G, Merkle H, Ellermann JM, Ugurbil K. Functional brain mapping by blood oxygenation level-dependent contrast magnetic resonance imaging. Biophys J. 1993; 64:800–812.

Padma MV, Bhasin A, Bhatia R, Garg A, Singh MB, Tripathi M, Prasad K. Normobaric oxygen therapy in acute ischemic stroke: A pilot study in Indian patients. Ann Indian Acad Neurol. 2011; 13:284–8. [PubMed: 21264137]

Santosh C, Brennan D, McCabe C, Macrae IM, Holmes WM, Graham DI, Gallagher L, Condon B, Hadley DM, Muir KW, Gsell W. Potential use of oxygen as a metabolic biosensor in combination with T2*-weighted MRI to define the ischemic penumbra. J Cereb Blood Flow Metab. 2008; 28:1742–53. [PubMed: 18545262]

Schlaug G, Benfield A, Baird AE, Siewert B, Lovblad KO, Parker RA, Edelman RR, Warach S. The ischemic penumbra: operationally defined by diffusion and perfusion MRI. Neurology. 1999; 53:1528–1537. [PubMed: 10534263]

Schmidt KF, Febo M, Shen Q, Luo F, Sicard KM, Ferris CF, Stein EA, Duong TQ. Hemodynamic and metabolic changes induced by cocaine in anesthetized rat observed with multimodal functional MRI. Psychopharmacology. 2006; 185:479–86. [PubMed: 16550388]

Shen Q, Meng X, Fisher M, Sotak CH, Duong TQ. Pixel-by-pixel spatiotemporal progression of focal ischemia derived using quantitative perfusion and diffusion imaging. J Cereb Blood Flow and Metab. 2003; 23:1479–1488. [PubMed: 14663344]

Shen Q, Fisher M, Sotak CH, Duong TQ. Effects of reperfusion on ADC and CBF pixel-by-pixel dynamics in stroke: characterizing tissue fates using quantitative diffusion and perfusion imaging. J Cereb Blood Flow Metab. 2004a; 24:280–90. [PubMed: 15091108]

Shen Q, Ren H, Bouley J, Fisher M, Duong TQ. Dynamic tracking of acute ischemic tissue fates using improved unsupervised ISODATA analysis of high-resolution quantitative perfusion and diffusion data. J Cereb Blood Flow and Metab. 2004b; 24:887–897. [PubMed: 15362719]

Shen Q, Ren H, Cheng H, Fisher M, Duong TQ. Functional, perfusion and diffusion MRI of acute focal ischemic brain injury. J Cereb Blood Flow and Metab. 2005; 25:1265–1279. [PubMed: 15858531]

Shen Q, Duong TQ. Quantitative Prediction of Ischemic Stroke Tissue Fate. NMR Biomed. 2008; 21:839–848. [PubMed: 18470956]

Shin HK, Dunn AK, Jones PB, Boas DA, Lo EH, Moskowitz MA, Ayata C. Normobaric hyperoxia improves cerebral blood flow and oxygenation, and inhibits peri-infarct depolarizations in experimental focal ischaemia. Brain. 2007; 130:1631–42. [PubMed: 17468117]

Sicard K, Shen Q, Brevard ME, Sullivan R, Ferris CF, King JA, Duong TQ. Regional cerebral blood flow and BOLD responses in conscious and anesthetized rats under basal and hypercapnic conditions: implications for functional MRI studies. J Cereb Blood Flow Metab. 2003; 23:472–81. [PubMed: 12679724]

Sicard KM, Duong TQ. Effects of Hypoxia, Hyperoxia and Hypercapnia on Baseline and Stimulus-Evoked BOLD, CBF and CMRO2 in Spontaneously Breathing Animals. NeuroImage. 2005; 25:850–858. [PubMed: 15808985]

Tanaka Y, Nagaoka T, Nair G, Ohno K, Duong TQ. Arterial spin labeling and dynamic susceptibility contrast CBF MRI in postischemic hyperperfusion, hypercapnia, and after mannitol injection. J Cereb Blood Flow Metab. 2010 in press.

Highlights

- This study characterizes the effects of transient OC on T_2^*-weighted MRI in permanent focal stroke rats.
- The ischemic core cluster showed no significant response, whereas the mismatch cluster showed markedly higher percent changes relative to normal tissue in the acute phase.
- The majority of the mismatch pixels showed exaggerated OC responses, which eventually infracted.
- OC-induced changes on the perfusion-diffusion contourplot dropped monotonously for pixels below perfusion and diffusion viability thresholds.
- Basal T_1 increased slightly in the ischemic core. OC decreased T_1 in normal but not mismatch and core pixels.
- OC decreased CBF in normal but not mismatch and core pixels.
- T_2^*-weighted MRI of OC has the potential to offer unique clinically relevant data.

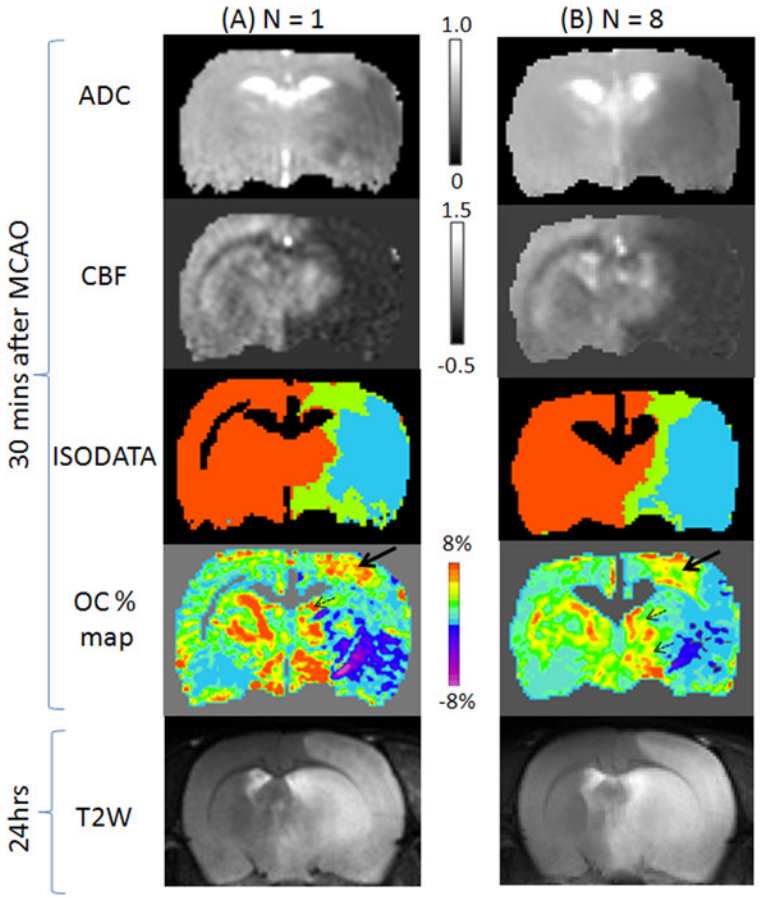

Figure 1.

(A) ADC, CBF, ISODATA and oxygen-challenge percent change maps at 30 mins after MCAO and T_2-weighted MRI at 24 hrs after MCAO from **(A)** one animal and **(B)** all 8 animals. Scale bar unit for ADC is 10^{-3} mm^2/s and for CBF is ml/gram/min. In the ISODATA maps, normal is shown as orange, mismatch as green, and core as cyan. Excluded CSF and corpus callosum are shown as black. Arrows indicate regions of exaggerated OC responses.

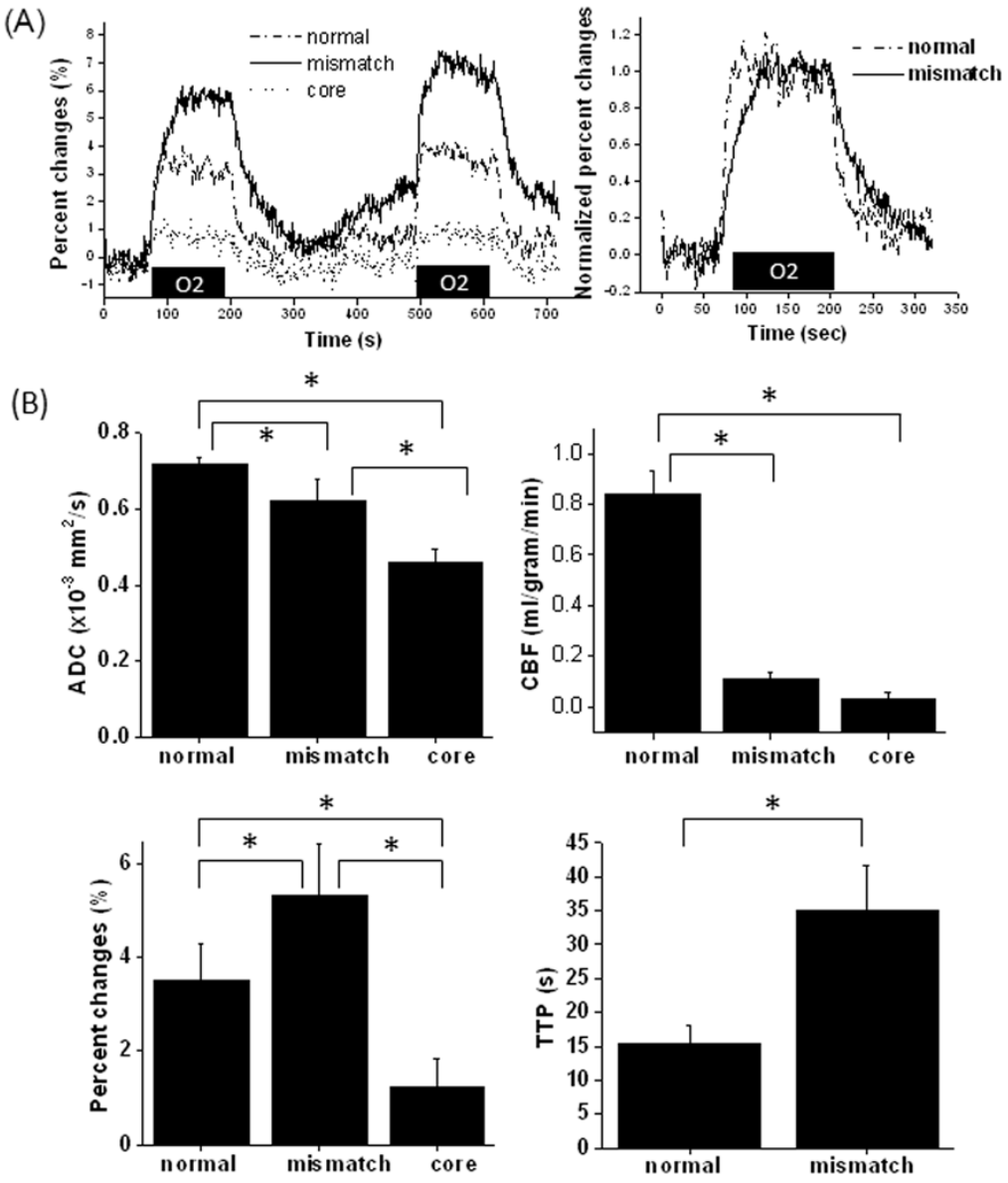

Figure 2.

(A) T_2^*-weighted MRI response time courses responding to transient oxygen challenge in three tissue types (core, mismatch and normal) from all animals, and the normalized group-averaged oxygen-challenge response time courses of the normal and mismatch pixels. **(B)** Group-averaged ADC, CBF, oxygen-challenge percent changes, time-to-peak (TTP) of the oxygen-challenge responses of three tissue types at 30 mins after stroke. Error bars are standard deviations for N = 8 and * indicates $P < 0.05$.

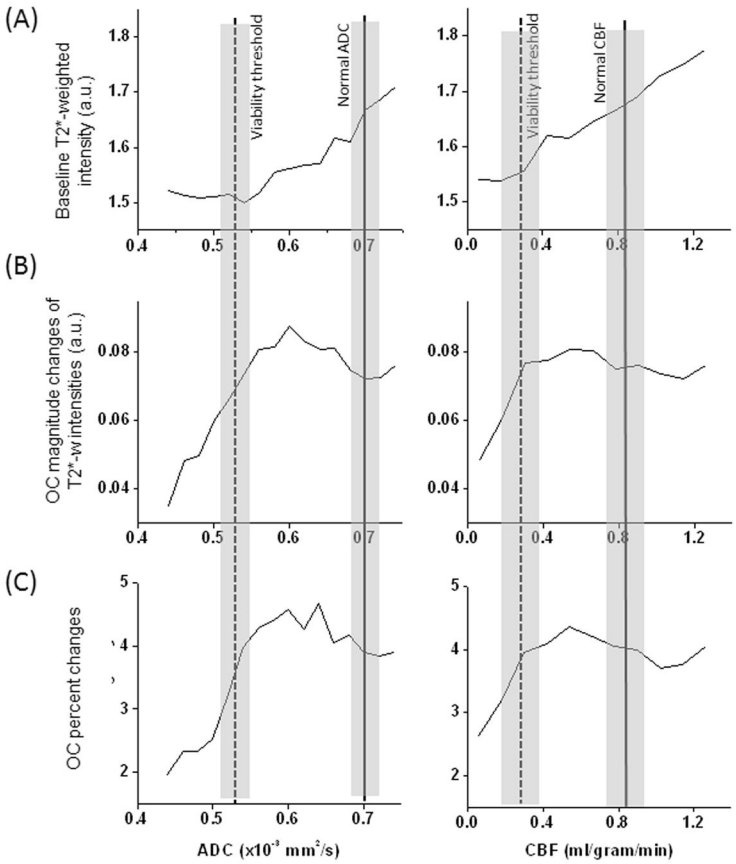

Figure 3.

(A) Group-averaged profiles of baseline T_2^*-weighted signal intensity, **(B)** magnitude changes in T_2^*-weighted intensity by oxygen challenge, and **(C)** percent changes by oxygen challenge as function of ADC and CBF at 30 mins after stroke. The vertical solid lines indicate normal ADC and CBF with shaded bars indicating their standard deviations from this study. Two vertical dot lines indicate the viability thresholds with shaded bars indicating their standard deviations as reported in (Shen et al., 2003).

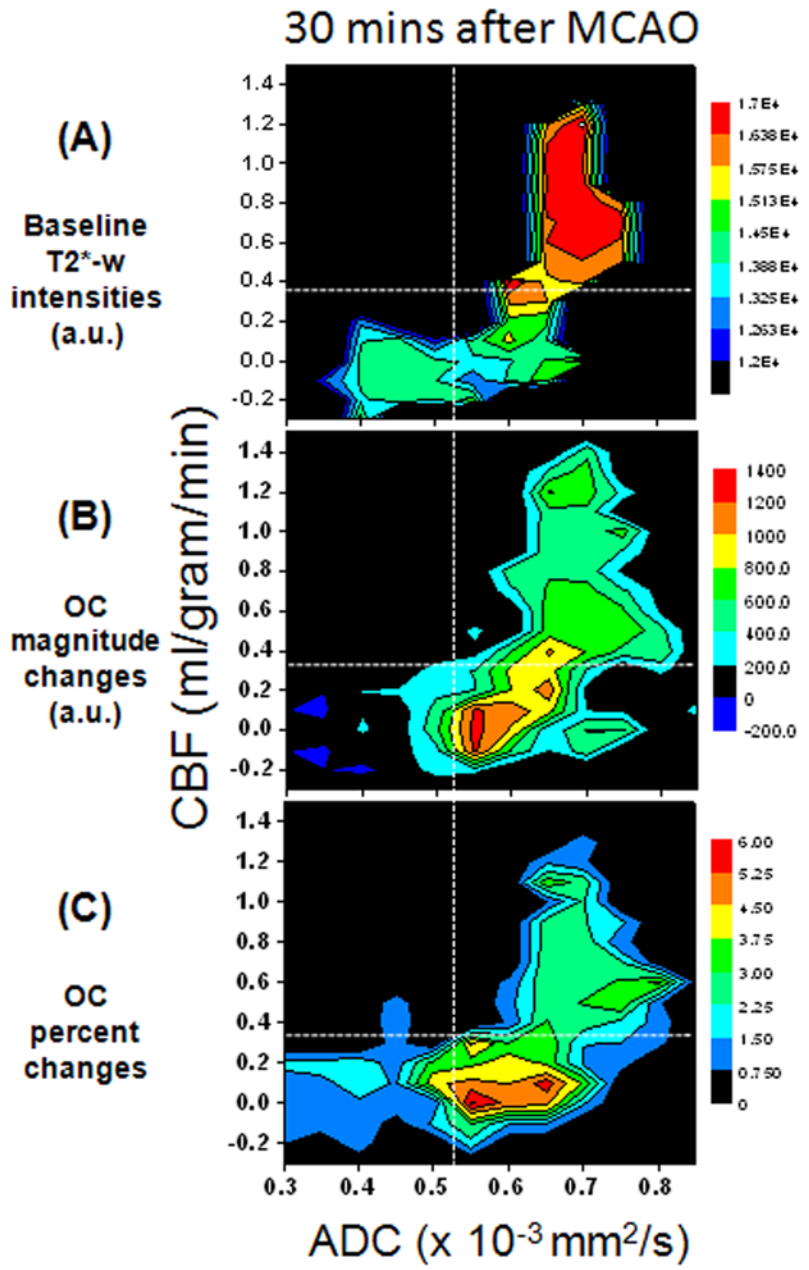

Figure 4.

(A) Group-averaged CBF-ADC contour plots of **(B)** baseline T_2^*-weighted signal intensity, **(B)** magnitude changes in T_2^*-weighted intensity by oxygen challenge, and **(C)** percent changes by oxygen challenge at 30 mins after stroke from whole-brain pixels. For reference, the vertical and horizontal dash lines indicating, respectively, the ADC and CBF viability thresholds are shown (Shen et al., 2003).

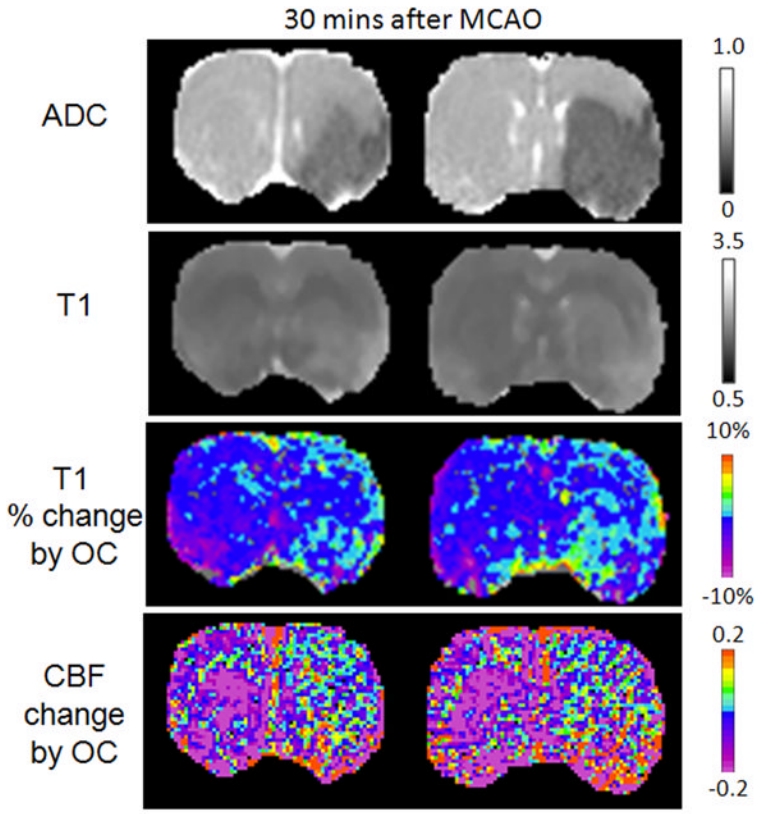

Figure 5.
ADC, baseline T_1, and T_1 change due to oxygen challenge and CBF change due to oxygen challenge at 30 mins after stroke. ADC is in unit of 10^{-3} mm^2/s and T_1 is in unit of s.